Renewable and Sustainable Energy Reviews 75 (2017) 1348–1362

Contents lists available at ScienceDirect

Renewable and Sustainable Energy Reviews

journal homepage: www.elsevier.com/locate/rser

The performance of some state-of-the-art wave energy converters in locations with the worldwide highest wave power

Liliana Rusu, Florin Onea*

"Dunarea de Jos" University of Galati, Department of Mechanical Engineering, Romania

ARTICLE INFO

Keywords:
World Ocean
Coastal environment
Wave power
ERA-interim data set
WECs

ABSTRACT

The main objectives of the present work are to review the global wave energy resources according to the most recent datasets available, to identify the locations with the worldwide highest wave energy potential and to assess in those locations the performance of some state-of-the-art wave energy converters. For this purpose, 15 years of wave data provided by the European Centre for Medium-Range Weather Forecasts, covering the time interval 2000–2014, were considered, processed and analysed. After identifying the geographical regions with the highest wave power, 15 reference points, which were considered more relevant from the point of view of their wave energy potential, have been defined in each hemisphere (northern and southern, respectively). As a following step, corresponding to all of these reference points, the most relevant wave patterns have been identified, and this information was subsequently used to assess the expected power output of the wave energy converters considered. Some other relevant parameters, such as the capacity factor or the capture width, were evaluated as well. Following the results provided by this work, we can expect that most of the existent devices for harnessing wave energy would perform well near most of the coastal environments identified. Moreover, it also must be highlighted that in the future, wave energy farms can play a very active role from the point of view of coastal protection.

1. Introduction

Marine areas are among the most sustainable environments from the point of view of energy potential. Historically, these areas have significantly influenced global economic growth through ship transport, and current technological developments recommend them as very competitive in the context of renewable energy resources. Another significant particularity of these areas is that in many cases, a single location can be used to capture various natural resources, such as wind, wave, tidal or thermal energy, through so-called hybrid farms [1–4]. At this moment, the research activities are focused on the coastal areas facing the oceans [5–9] and also on some enclosed seas that have some hotspot areas with relevant wind and wave energy potential, as in the case of the Mediterranean, Black and Caspian seas [10–17].

Most renewable sources are related to the energy radiated by the sun; this is also the case of wave energy, which in many cases is associated with a more concentrated form of solar energy because on a large scale, the gradual heating of the earth releases a considerable amount of energy on the air–sea interface, generating the wind and the waves. At this stage, capillary waves are generated, and under favourable wind conditions, they can grow to consistent surface gravity waves (swell), which are interesting for the Wave Energy Converter (WEC) industry owing to their high energy density [18]. The World Ocean is composed of five major oceans (Antarctic, Arctic, Atlantic, Indian and Pacific), in which the best energy resources can be found on the western coasts of the continents, especially between 30° and 60° latitude in both hemispheres [19,20]. However, the Antarctic and Arctic environments cannot be considered suitable for wave energy extraction owing to the extreme conditions reported in these areas, although at this moment, there are several projects focused on this issue [21,22]. From the coastal regions, a particular case is represented by the islands and archipelagos [23–25], which may represent important sources of wave energy because they are located in deep water areas (with steep shorelines) and thus present the opportunity to capture a large amount of wave energy before the dissipation processes between the waves and the sea bottom begins to occur [26].

Because the oceans cover almost 71% of the Earth's surface, it is difficult to assess in detail the wave conditions with in situ instruments, especially regarding offshore areas. In this case, a viable alternative is to consider simulated data from various numerical models, which are constantly calibrated with measurements provided by the satellite missions, research ships or data from buoys and coastal stations. The

* Corresponding author.
E-mail address: florin.onea@ugal.ro (F. Onea).

http://dx.doi.org/10.1016/j.rser.2016.11.123
Received 5 August 2015; Received in revised form 12 May 2016; Accepted 9 November 2016
Available online 17 November 2016
1364-0321/

benefits of these blended datasets are that they are available on a global scale, they report no gaps in the time series, and they are defined by good spatial and temporal resolution. Another advantage comes from the fact that these databases cover long periods of time, as in the case of the European Centre for Medium-Range Weather Forecasts (ECMWF) [27], which provides reliable information about the wind and wave conditions starting in 1979.

Similar to wave motion, the WEC industry has had many ups and downs starting in 1799 when Girard and his son patented their work in France [28]. It is estimated that almost 150 WEC projects (either conceptual or operational) have been reported at a global scale compared with the offshore wind industry, which the classical wind turbine is combined with various offshore foundations. Among these, more than 50% of WECs were developed in Europe (especially in the United Kingdom) [29,30], with point absorber devices being among the most researched systems. Outside Europe, the US reports the most intense activity (with 33 concepts), whereas the opposite case can be found in countries such as Chile, Mauritius and New Zealand although they have excellent wave conditions. The interest in wave energy is obvious [31–34] if we consider that at this moment there will soon be 16 operational sites, where the resources may vary from 3 kW/m to 50 kW/m, from which we can mention DanWEC (Denmark), EMEC (Scotland) or HINMREC (Hawaii).

Because there is a strong connection between wind and wave conditions, to accelerate the implementation of WECs, a possible solution will be to use the existing offshore wind farm infrastructure to reduce the costs and to increase the availability of a location by compensating for the variability of the wind conditions [35–38]. Moreover, wave farms also represent a viable solution for coastal protection in the case of coastal sectors affected by strong erosion processes [39–42].

Motivated by these aspects, the present work aims to evaluate the global wave energy potential in various locations where wave energy is considered to be abundant and to assess the performance of some state-of-the-art WEC systems in terms of their expected energy production or efficiency parameters. The main original feature of this work is in the fact that for the first time, many WEC devices are considered for such a study, considering conversion systems that cover a wide range of rated powers; moreover, this evaluation is carried out on a global scale.

2. Methods and materials

2.1. ERA-Interim global wave data

One of the most complete environmental databases is produced by the European Centre for Medium-Range Weather Forecasts (ECMWF), from which the ERA-Interim project stands out as a high-quality reanalysis dataset capable of describing various parameters from the marine environment, such as wave and wind conditions, ice temperature and solar radiation. The ongoing project covers almost 35 years of data (1979–present), defined by a spatial resolution that may vary from 0.125 to 3° and a temporal resolution of 4 data per day (corresponding to 00–06-12–18 UTC).

The ECMWF version of WAM (Wave Modelling) is capable of assessing various wave characteristics from the two-dimensional wave spectrum $F(f, \theta)$ [43]. In this way, the total wave energy is represented as a function of frequency (f) and direction (θ). The (n)-order moment of the spectrum (m_n) and the 1-D frequency spectrum $E(f)$ can be defined as follows:

$$m_n = \int df d\theta f^n F(f, \theta) \quad (1)$$

$$E(f) = \int d\theta F(f, \theta) \quad (2)$$

Subsequently, the significant wave height (Hs) can be expressed as

$$Hs = 4\sqrt{E_0} \quad (3)$$

where E_0 is the wave energy ($E_0 = m_0$).

The mean wave period T_{-1} (denoted in this work as Te, and called also the wave energy period) is related to the spectral moments as follows:

$$T_{m-1} = \frac{m_{-1}}{m_0} \quad (4)$$

Finally, the mean wave direction (°) can be defined as $\langle\theta\rangle = a\tan(SF/CF)$, where SF and CF are the integrals of $\sin(\theta)F(f, \theta)$ and $\cos(\theta)F(f, \theta)$, respectively.

An important step in the numerical process is represented by the assimilation scheme of the wave data and the accuracy of the sources. Initially, the ECMWF model used the altimeter wave height observations provided by ERS-1 and ERS-2 (1993–2003) as the input, and in 2003, the satellites ENVISAT and Jason were added for operational analysis. Although the altimeters provide relatively accurate information about the wind and wave conditions, the small footprint of the altimeters represents a drawback because only small regions (along the tracks) can be investigated. As previously mentioned, a more accurate description of the sea states can be achieved by considering the two-dimensional wave spectrum; this principle already being used by the synthetic aperture radar (SAR), which can easily cover an ocean footprint of 100 km, as in the case of the ENVISAT ASAR missions. A complete description of the ECMWF wave model can be found in some relevant works, which are focused more on the technical aspects [44,45].

In the framework of the present work, the ERA-Interim dataset was processed on a global level considering a spatial resolution of 0.75°×0.75°, with results reported in the 15-year time interval from January 2000 to December 2014.

2.2. Wave power potential of the World Ocean

Fig. 1 presents the distribution of the mean wave power density, Pw (kW/m); this parameter is defined as

$$P_W = \frac{\rho g^2}{64\pi} T_e H_s^2, \quad (5)$$

where P_W is the energy flux per meter of the wave crest (kW/m), ρ=1025 kg/m^3 is the density of the seawater, and g is the acceleration due to gravity.

Based on the ERA-Interim dataset, the global map was designed for the entire 15-year interval of 2000–2014, including the areas from the Northern and Southern hemispheres covered by ice. As expected, more consistent wave power potential is encountered in the areas located between the 40° and 60° latitude lines (north and south), noting that a maximum of 127.7 kW/m is encountered in the Indian Ocean region. Because only the coastal environments currently present real interest for wave energy extraction, this category can include the southern part of Australia and some regions from Europe, where the wave power can reach values in the range of 70–80 kW/m. In addition to these areas some hotspots in the southern extremities of South America or Africa can also be mentioned, although there currently are no public plans to exploit this source of energy in those regions. It also must be highlighted that the mean values presented in this map appear to be in agreement with some other works, which are related to various other data sources, as in the case of the UK ~75 kW/m [46]; southern Madagascar →25–50 kW/m [47]; the Indian Ocean ≈120 kW/m [31] and Peru ≤25 kW/m [48].

To assess the expected performance of some state-of-the-art wave energy converters, thirty reference points were considered for further analysis, whose distributions were equally divided between the northern and southern hemispheres. As Fig. 1 illustrates, group points A1–A6 are located near the western coast of the American continent and

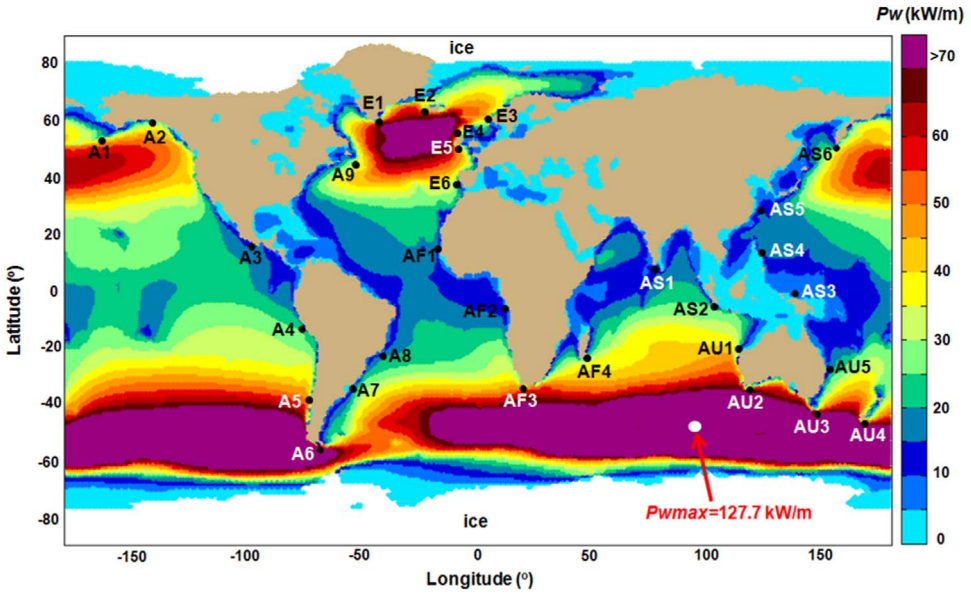

Fig. 1. Map of the mean wave power density (in kW/m) corresponding to the 15-year interval from January 2000 to December 2014; the positions of 30 reference points, distributed along the coastal environments of: America (A1–A9), Europe (E1–E6), Africa (AF1–AF4), Asia (AS1–AS6) and Australia (AU1–AU5), are also indicated.

are under the influence of waves coming from the Pacific Ocean. Points A7–A9 are located near the eastern coast, more precisely between Uruguay and Canada. Near the European coasts, reference points E1–E6 have been defined, which are near the shorelines of Greenland, Iceland, Norway, the UK and Portugal.

Around the African coasts, points AF1–AF3 were defined. In this region, point AF4 was also included, which was selected in the southern extremity of Madagascar Island. Further to the east, reference points AS1–AS6 were defined, which correspond to the Asian region. As Fig. 1 illustrates, half of these points are located in the vicinity of some important islands, as in the case of AS3 (near Papua New Guinea). This list is completed with points AU1–AU5 in the western Australian coastal environment, which will encounter waves generated in the Indian Ocean. From these last reference points, AU4 can be mentioned. This was selected in the southern extremity of the Tasmanian islands.

Some further details about the reference points selected above can be found in Table 1. All points were defined in deep water areas, which may vary from 42 m (AU5) to 170 m (AS3), and in terms of the distance from shore, a minimum of 4.2 km can be mentioned for AF1 and a maximum of 236 km for AS5. Owing to the considerable distance from the shoreline, points AF1 and A9 represent a less attractive solution for a wave farm project because the initial investments can be quite substantial. Nevertheless, these points can present interest in the future if we consider that at this moment, there are plans to develop offshore wind farms at distances 200 km from the shore and depths of 215 m [49].

2.3. Wave Energy Converters (WECs)

According to their working principles, the operating WEC devices can be placed in three distinct categories: point absorbers, attenuators and terminators. In the first case, the system is similar to a buoy, in which the active part moves on a vertical axis. The second system is oriented along the wave direction, gradually generating energy as the wave passes through the system length, compared with the terminator devices that act as breakwaters. In Table 2, the main features of the ten

Table 1
Locations and main characteristics of the sites (30 reference points) considered for evaluation.

Pt.	Location (Long-Lat)	Depth (m)	Distance to shore (km)	Pt.	Location (Long-Lat)	Depth (m)	Distance to shore (km)	Pt.	Location (Long-Lat)	Depth (m)	Distance to shore (km)
A1	53°57'N 164° 8'W	74	56.8	**E2**	63°39'N 23°14'W	106	31.6	**AS2**	5°12'S 103°38'E	98	22.5
A2	59°50'N 142°20'W	106	24.6	**E3**	61°51'N 4°31'W	137	16.1	**AS3**	3°2'S 142°15'E	170	6.7
A3	16°12'N 98°34'W	96	13.4	**E4**	55°52'N 8°29'W	134	87.8	**AS4**	13°58'N 124°27'E	74	11.1
A4	13°N 76°42'W	97	21.4	**E5**	50°11'N 8° 2'W	103	159	**AS5**	28°15'N 124°5'E	90	236
A5	39°26'N 73°37'W	105	35.3	**E6**	37°40'N 8°55'W	98	10.3	**AS6**	50°46'N 157°6'E	79	27
A6	56° 1'S 68°36'W	101	49.2	**AF1**	14°44'N 17°35'W	108	4.2	**AU1**	21°24'S 114°26'E	131	55.2
A7	35°58'S 54°46'W	97	114	**AF2**	6°28'N 11°56'	93	56.7	**AU2**	35°23'S 117°57'E	102	28.6
A8	23°10'S 41°34'W	94	49.4	**AF3**	35° 8'S 20°16'E	119	41.6	**AU3**	43°52'S 146°44'E	72	29.2
A9	44°48'N 53°15'W	101	206	**AF4**	25°19'S 46°57'E	72	28.36	**AU4**	46°12'S 166°25'E	162	16.2
E1	59°46'N 42°56'W	146	20.5	**AS1**	7°37'N 77°33'E	73	53.7	**AU5**	24°48'S 153°25'E	42	17.3

Table 2
Technical specifications of the 10 WEC systems considered in the present work [50–63].

Category	Device type	Dimensions	RP (kW)	Projects to Date	Ref.
Point absorber	Pontoon Power Converter (PPC)	80 m	3619	R & D phase	[50][51]
	Ocean Energy Buoy (OE)	50 m	2880	R & D phase (1:4 scale model)	[51]
	Wave Bob	20 m	1000	R & D phase (1:4 scale model)	[51]
	Ceto	7 m	260	● Garden Island, Western Australia ● Wave Hub, Cornwall, UK *Pre-consented (3 MW each project)	[51][52]
	SeabasedAB	3 m	15	Sotenäs, Sweden. *Pre-consented—10 MW demonstration plant	[53–55]
Attenuator	Sea Power	16.75 m	3587	Galway Bay, Ireland—test site	[56][57]
	Wave Star	70 m	2709	Hanstholm, Denmark (1:2 scale model—600 kW machine)	[58][58]
	Pelamis	150 m	750	● Agucadoura, Portugal (2.25 MW project) *Company—Financial problems	[59][60]
	Oceantec	52 m	500	Sea trials—1:4 scale model	[61][62]
Terminator	Wave Dragon	–	5900	Nissum Bredning, Denmark—prototype testing	[60][63]

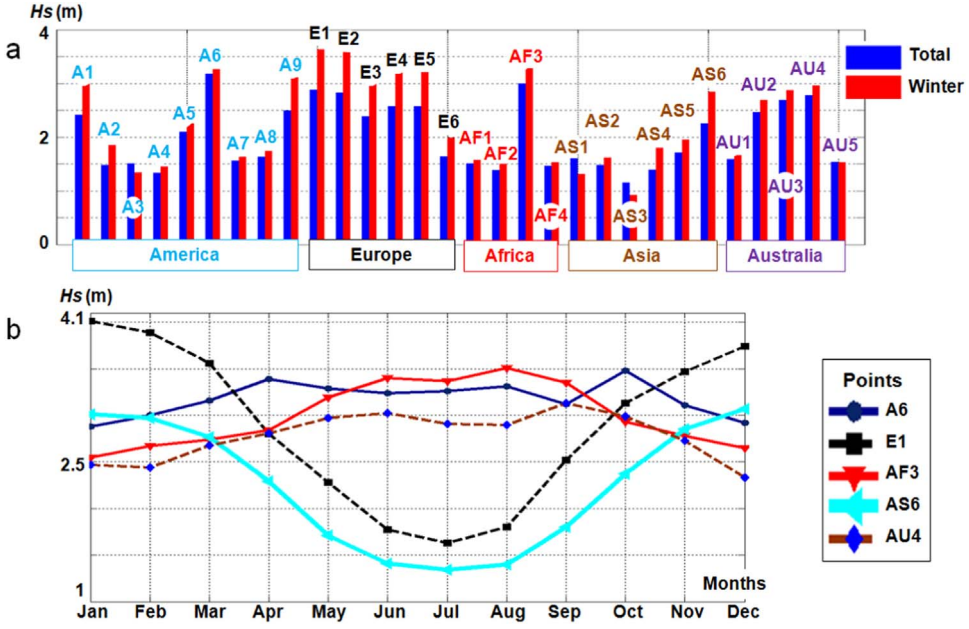

Fig. 2. Average *Hs* values corresponding to the 15-year time interval from January 2000 to December 2014: a) values corresponding to the total and winter times; b) *Hs* monthly variations corresponding to the most energetic sites in each continental area. For the Northern Hemisphere, wintertime represents the period between October and March, whereas for the Southern Hemisphere, wintertime is the period between April and September.

Table 3
Main characteristics of the wave conditions corresponding to the most energetic locations from the reference points considered in the vicinity of each continent. The results cover the 15-year interval from January 2000 to December 2014, structured on total and winter times, respectively.

Point	*Hs* (m)		*Hs* (m)—95th		> 3 m (%)		*Te* (s)		*Te* (s)—95th		*Pw* (kW/m)		*Pw* (kW/m)—95th	
	TT	WT	TT	WT	TT	WT	TT	WT	TT	WT	TT	WT	TT	WT
A6	3.18	3.27	5.32	5.51	49.9	52.3	9.2	9.41	11.3	11.6	52.6	57	138	150
E1	2.88	3.63	5.6	6.26	38.5	61.5	8.7	9.5	11.3	11.8	47.4	72.5	158	205
AF3	3	3.28	4.81	5.23	40.6	52.4	9.99	10.4	12.4	12.7	49.2	60.7	123	149
AS6	2.25	2.84	4.65	5.25	21.3	36.3	8.11	8.58	10.6	11.1	27.6	42.3	101	133
AU4	2.78	2.96	4.58	4.86	34.1	40.6	8.52	8.81	10.4	10.7	36.3	42.1	94.5	110

WEC systems considered for analysis are presented, in which five point absorbers, four attenuators and one terminator can be found. Regarding the point absorber systems, it can be mentioned that although the Wave Star and Pontoon were included in this category, they are defined in fact by multiple point absorbers mounted on a fixed structure, which—depending on the dominant wave direction—may act as "pseudo-attenuators" or "pseudo-terminators". As an example, the Wave Star system has a total length of approximately 70 m, although each individual buoy has a diameter of 5 m.

According to their rated power (denoted as *RP* in kW), we can group the selected systems into two categories: a) systems rated above 2500 kW and b) systems rated below 1000 kW. For each system, the *RP* parameter was defined as the maximum value reported in the power matrix available for each WEC; this aspect is presented in further detail in the forthcoming sections. At this point, it should also be mentioned that the immaturity of this industry can be observed from the fact that most systems are still at the Research & Development (R & D) stage: some of the devices are still being tested in the harsh ocean environ-

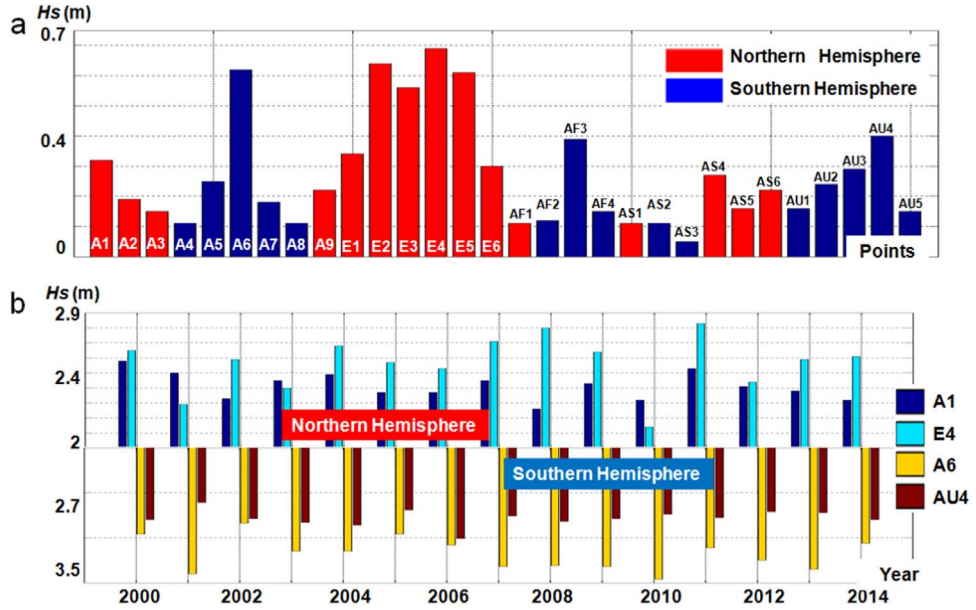

Fig. 3. Inter-annual variation of the *Hs* parameter corresponding to the 15-year time interval from January 2000 to December 2014: a) *Hs* differences corresponding to each point; b) annual distribution of the *Hs* values for points A1, E4, A6 and AU4.

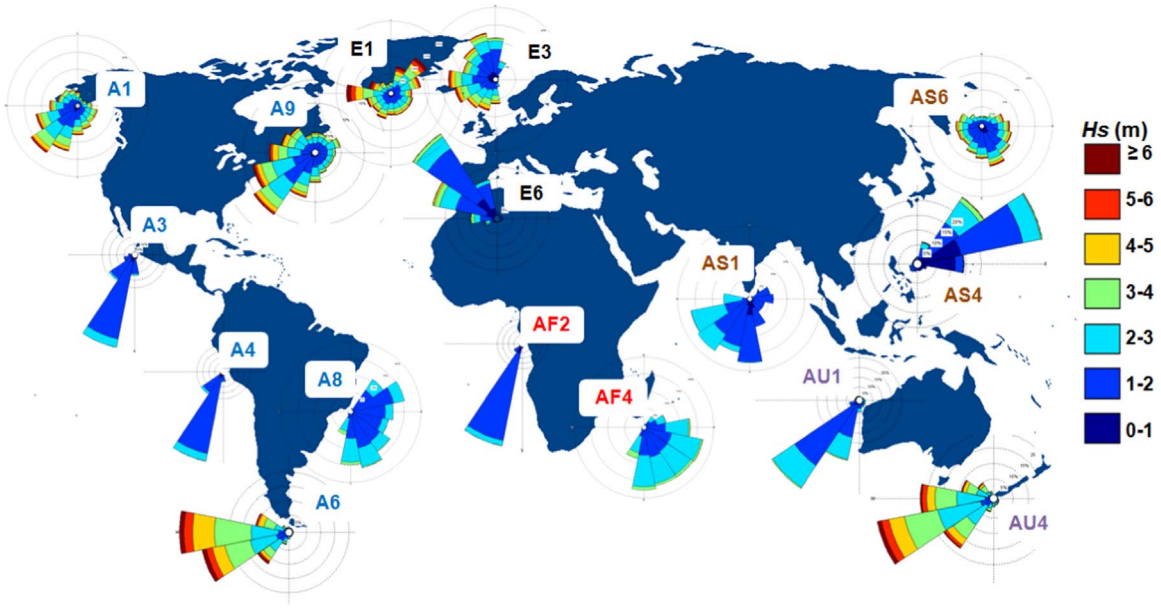

Fig. 4. Wave rises corresponding to the 15-year interval from January 2000 to December 2014, considered for the total time period only.

ment, whereas other projects are in standby, as in the case of the Pelamis system, which is currently encountering financial problems. Nevertheless, in this way, by considering a large variety of devices (in a power range from 15 kW to 5900 kW), it is possible to identify the performance of most offshore WEC systems available in the market to assess which system would be more suitable for a particular geographical area. Regarding the Wave Dragon system, the analysis is based on the results available in some previous works, which do not mention the dimensions of this system.

3. Results

3.1. Analysis of the wave power distribution

In Fig. 2a, the distribution of the parameter *Hs* (mean values) for the interval 2000–2014 is structured in both total and winter times. In the case of the Northern Hemisphere, the wintertime is associated with the time interval of October–March, whereas in the Southern Hemisphere, this is the period of May–September. As we can see, higher values are encountered during wintertime, with the exception of points A3, AS1 and AS3. In this category, we can also include point AU5, which does not register any significant variation. During the total time, the points present mean *Hs* values in the ranges A4–A6 (1.33–3.18 m), E6–E1 (1.64–2.88 m), AF2–AF3 (1.38–3 m), AS3–AS6 (1.15–2.25 m) and AU5–AU4 (1.54–2.78 m), whereas for the wintertime, the maximum values of E1 (3.63 m), AF3 (3.28 m), A6 (3.27 m), AU4 (2.96 m) and AS6 (2.84 m) can be observed.

Fig. 2b presents the monthly distribution of the *Hs* mean values for the reference points of each continent, which seem to present the higher values. The differences between the Northern and Southern Hemispheres are obvious: points E1 and AS6 located in the northern part more clearly show the differences between the summer and winter times compared with the other points that present only small variations. From the northern region, point E1 presents a maximum of 4 m

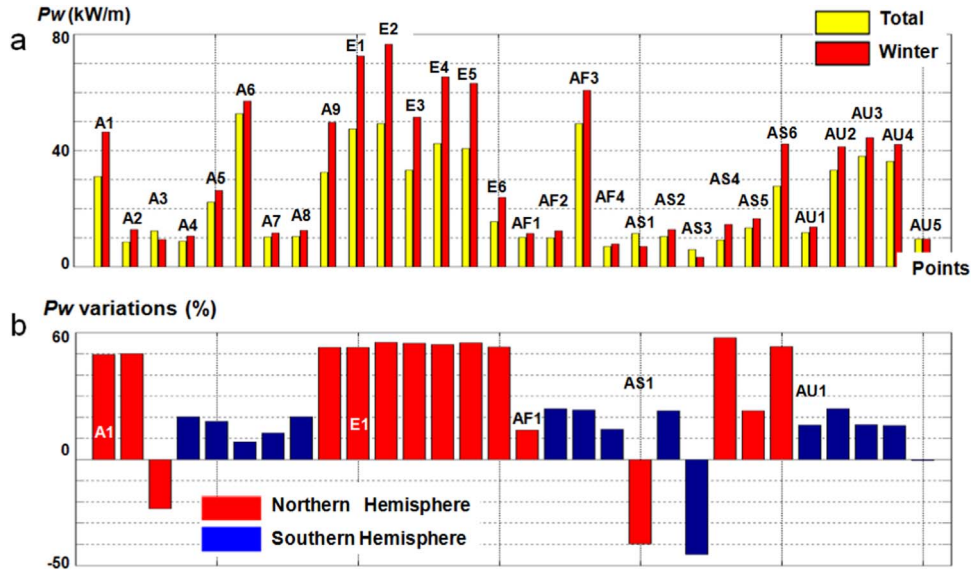

Fig. 5. Wave power corresponding to the 15-year interval from January 2000 to December 2014, structured on total and winter time: a) the energy flux in kilowatts per meter of the wave crest (kW/m); b) relative variations between the winter and total times (expressed in %) reported to the total time interval. .

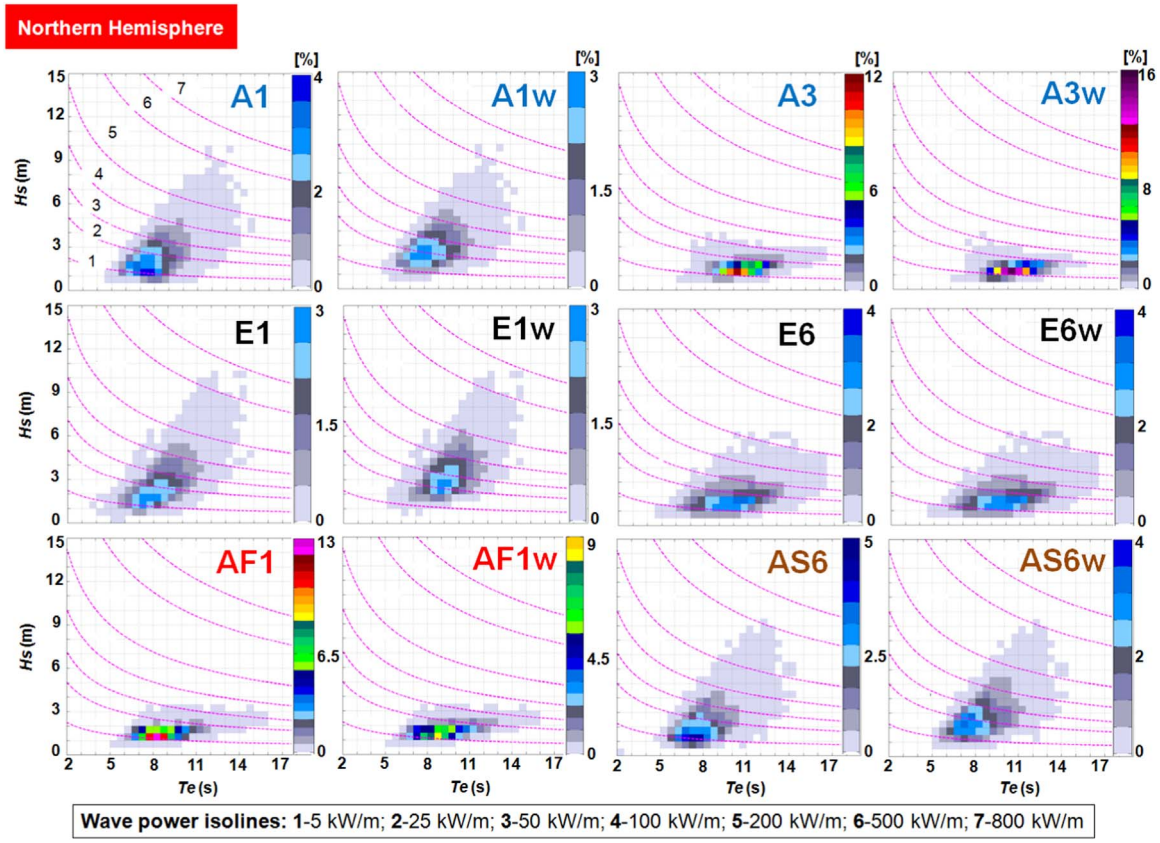

Fig. 6. Bivariate distributions of the parameters *Hs* and *Te* corresponding to six reference points from the Northern Hemisphere. Sea states corresponding to the 15-year interval from January 2000 to December 2014, structured in total and winter times (indicated throughout the subscript *w*). The wave power isolines were designed for seven energetic levels (from 1 to 7), where the higher values correspond to more energetic conditions.

in January and a minimum of 1.6 m in July compared with point AS6, which has values in the range of 1.34–3 m. The *Hs* values corresponding to points A6, AF3 and AU4 do not exceed 3.5 m, with the mention that point AU4 presents the lowest monthly average values.

A complete description of the wave characteristics is presented in Table 3, considering the reference points from Fig. 2b and the average values and the 95th percentiles of the following wave parameters: significant wave height—*Hs* (m), wave energy period—*Te* (s) and wave power density—*Pw* (kW/m). The mean values of the *Hs* parameter were already presented in Fig. 2b, from which it can be noted that during the total time, point A6 presents a maximum value of the average *Hs* of 3.18 m, compared with the winter time when point E1 has a maximum of 3.63 m. The 95th percentile (denoted as 95th) values are divided between points AU4 and E1, which for the total time may have values in the range of 4.58–5.6 m, whereas in winter, a maximum of 6.26 m is noticed in E1. The wave conditions are also

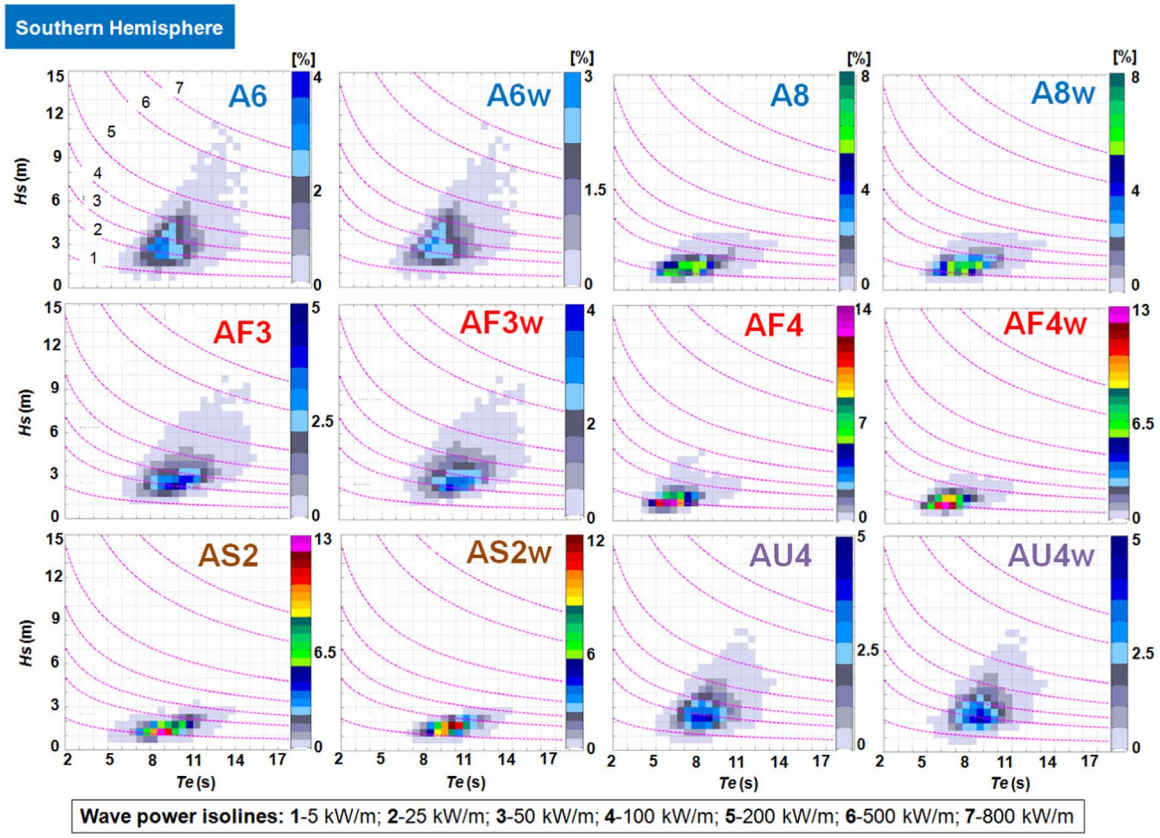

Fig. 7. Bivariate distributions of the *Hs* and *Te* parameters corresponding to six reference points from the Southern Hemisphere. Sea states corresponding to the 15-year interval from January 2000 to December 2014, structured in total and winter times (indicated throughout the subscript *w*). The wave power isolines were designed for seven energetic levels (from 1 to 7), where the higher values correspond to more energetic conditions.

analysed by reporting their distribution (in %) to the value of 3 m, from which we can notice that point A6 presents a maximum of 50% during the total time compared with 61.5% corresponding to point E1. This point is defined by the maximum variation between the total and winter times (23%).

The *Te* parameter presents small variations between the total/winter intervals, with average values of 8.11 s in AS6 and 10 s for AF3 during the total time, whereas a maximum 95th value of 12.7 s is noticed in the vicinity of the southern African coasts (point AF3). Regarding the wave power, we can notice that the mean values are much smaller than those indicated in Fig. 1 because although the selected points are located in areas with consistent energy potential, they were defined in the vicinity of the shoreline areas, which are under the influence of the dissipative processes. Thus, we can notice values of 52.6 kW/m in A6, 49.2 kW/m in AF3 and 36.3 kW/m in AU4 during the total time, whereas in winter, points AS6 and E1 can reach values of 42.3 kW/m and 72.5 kW/m, respectively. More significant values are seen in the 95th percentile, particularly for point E1, which reports a value of 205 kW/m, compared with AU4 where only a value of 110 kW/m is noticed.

In addition to the seasonal variations, most of the marine areas also present inter-annual variations, which could significantly influence the performance of the WEC systems, especially if the generators are installed in large-capacity wave farms. In Fig. 3a, such variations are presented for all reference points, where the values are computed as the mean annual differences between the minimum and the maximum values for all years corresponding to the interval of 2000–2014. We can also notice that European points E2–E5, located in the Northern Hemisphere, present more significant variations, which can reach a maximum value of 0.64 m. Point A6 (in the south) can also be mentioned, where a variation of 0.62 m is noticed. Other relevant points are AF3 and AU4, which show values close to 0.4 m, whereas almost half of the considered reference points present values below 0.2 m. A detailed investigation of the annual distribution of the *Hs* parameter (mean value) is presented in Fig. 3b for the points that present the most severe variations. Except for point AU4, which seems to have a more constant distribution of the values, the rest of the points present a cyclic distribution of the values with periods of one or two consecutive years, in which the wave conditions can have higher or lower values. For example, in the case of reference point E4, we can notice that there is a tendency for the wave energy to increase if we consider that the interval of 2007–2009 was among the most energetic with annual average *Hs* values in the range of 2.64–2.8 m, which were exceeded by a value of 2.83 m encountered in 2011. Although the variations illustrated in Fig. 3a are much smaller for the Southern Hemisphere, this region presents higher annual values, which can reach, for example, a maximum of 3.46 m in the case of reference point A6 (in 2010).

Another important parameter for a wave energy project is the wave direction. This is represented in Fig. 4 for all reference points and corresponds to the entire time interval considered (2000–2014). From the analysis presented in this figure, we can notice that the points located near the western coast of America indicate the Pacific Ocean as the main generation area, an aspect that is also highlighted by point AS4 defined on the north-eastern side of the Philippine Islands. Regarding the Indian Ocean, the swell spreads out in all directions reaching Madagascar (A4), Sri Lanka (AS1) or Australia (AU1 and AU4), whereas the European points encounter waves from the North Atlantic Ocean, noting that point E3 (Norway) can also encounter waves from the Arctic Ocean. From the analysis of the *Hs* distribution, we can notice that points A6, A9, E1 and AU4 present more frequent wave heights that exceed 6 m.

If we now relate the wave rises to the WEC classification presented in Table 2, we can notice that the point absorber systems are unaffected

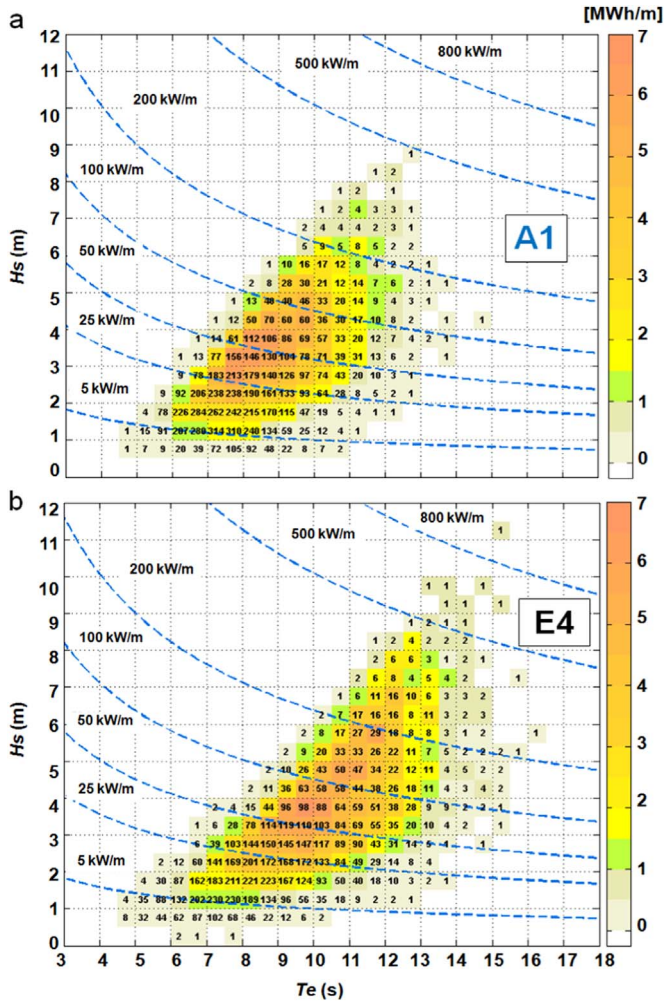

Fig. 8. Characterization of the wave energy resources at study sites A1 (a) and E4 (b) located in the Northern Hemisphere. For each combination of significant wave height (*Hs*) and energy period (*Te*), the colour indicates its contribution to the annual energy, whereas the numbers represent the occurrence (in number of hours in an average year). The wave power isolines are also represented.

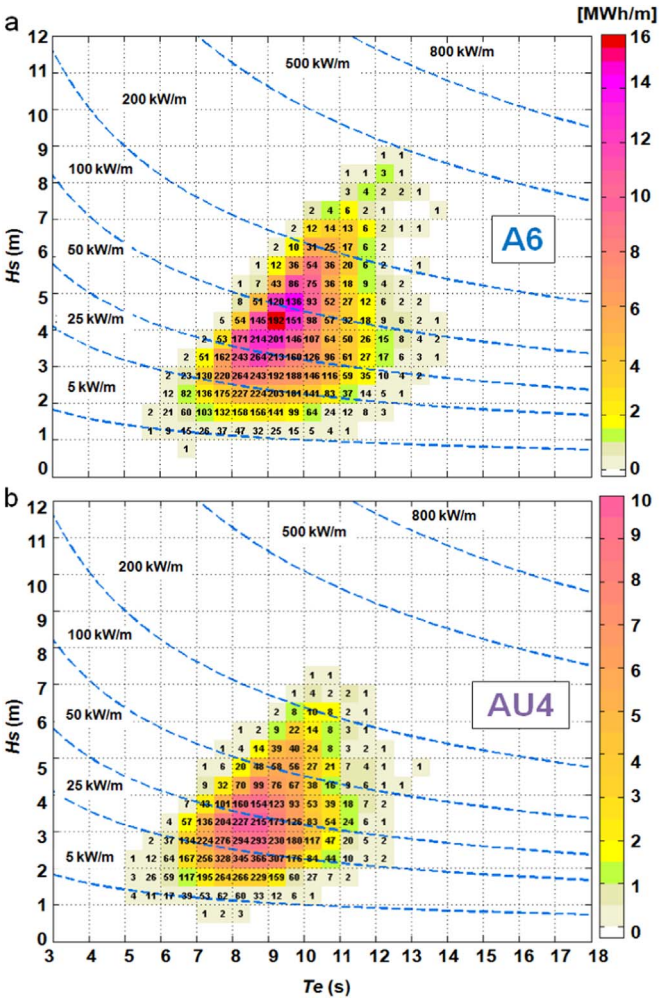

Fig. 9. Characterization of the wave energy resources at the study sites A6 (a) and AU4 (b) located in the Southern Hemisphere. For each combination of significant wave height (*Hs*) and energy period (*Te*), the colour indicates its contribution to the annual energy, whereas the numbers represent the occurrence (in number of hours in an average year). The wave power isolines are also represented.

by a wide directional distribution, a characteristic that could be associated with the points from the Northern Hemisphere. The attenuator and terminator type devices appear to be more suitable for areas with narrow distributions, as in the case of points A4, AF2 or AU1.

The distribution of the parameter *Pw*, presented in Fig. 5, more clearly shows the differences between the two hemispheres. At this point, it should also be mentioned that the wave power values presented in Fig. 5 could significantly change if we consider that the density of the water increases with decreasing ocean temperature. For this work, an average value of 1025 kg/m^3 was considered for all reference points. The results are defined according to the total and wintertime periods, including the variations reported between the two intervals (Fig. 5b), which were expressed in % while taking as references the *Pw* values corresponding to the total time. From these values, we can notice that the points from the Northern Hemisphere present more significant variations, which can reach 57.6% for AS4 or 55.2% for E2, whereas from Southern Hemisphere, points AF1, AF2, AS2 or AU2 can reach a maximum of only 24%. The less energetic winter season is obvious in the case of points A3, AS1 and AS3, where values can be reported in the range [−23.2, −45%].

The joint distribution of *Hs* and *Te* can be associated with a "fingerprint", which provides detailed information about the sea state of a specific location. These diagrams, also known as bivariate distributions, are based on 0.5 m×0.5 s cells ($\Delta Hs \times \Delta Te$), with results expressed as a percentage of the total occurrences. These types of distributions are important because they will have a significant role in the assessment of WEC performance.

Such an analysis is presented in Fig. 6 for several points from the Northern Hemisphere, the results of which are related to the entire time interval considered (2000–2014) and computed for the total and winter times, where the winter was indicated by the subscript w. In addition, in each subplot, the wave power isolines were included. These were denoted from 1 to 7, with higher values associated with a more energetic sea state. Points A3 and AF1 present a flattened distribution of the cells, with a significant amount of values between the isolines 5–25 kW/m and some cells with percentages between 12–13% from the total time. During wintertime, these distributions remain quite similar, noting that point A3 presents cells with 16%, compared with AF1, where the values decrease to a maximum of 9%. As expected, more important values occur in the reference point E1, where most of the distributions are centred in the ranges of 1–3 m and 6–10 s, whereas during wintertime, these distributions are focused on higher *Hs* and *Te* values. A similar pattern is observed for point AS6, noting that during the total time, the most important values are between the isolines 5–25 kW/m, values that can increase to 50 kW/m.

A similar diagram is presented in Fig. 7 for six reference points from the Southern Hemisphere, including A6, AF3 and AU4, which

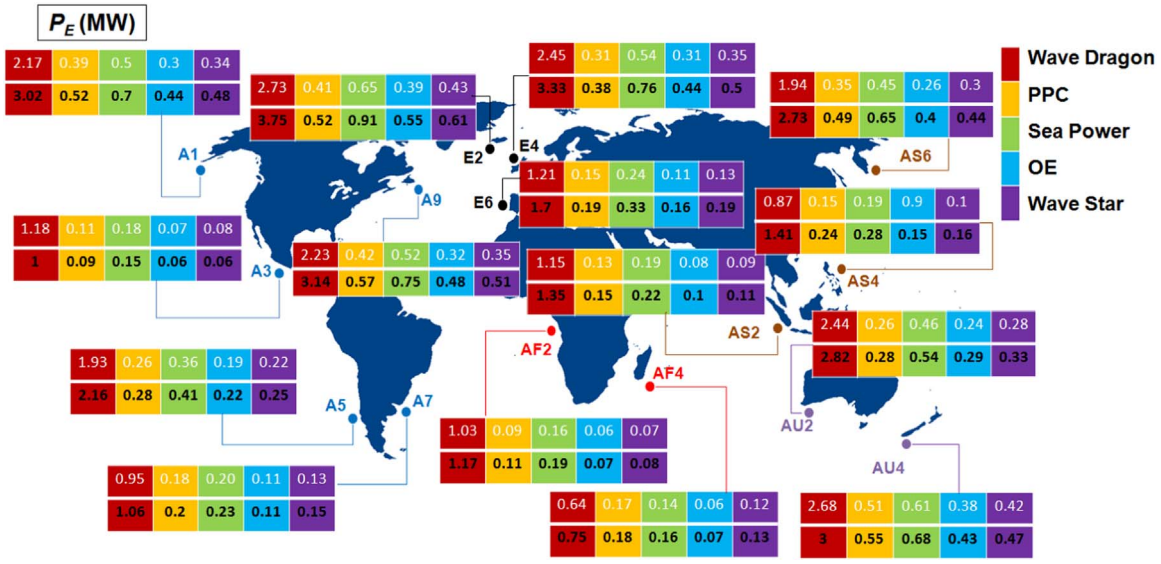

Fig. 10. Power output (in MW) expected from the WECs rated above 2500 kW. Mean values correspond to the 15-year interval from January 2000 to December 2014, where the first and second lines of each table indicate the WEC performance during the total and winter times, respectively.

Table 4
Power output (in MW) expected from the WECs rated above 2500 kW, indicated in terms of the mean values corresponding to the 15-year interval from January 2000 to December 2014, where the wintertime values are highlighted.

Point		Wave dragon		PPC		Sea power		OE		Wave star	
A2	**AF3**	0.6	3.24	0.15	0.39	0.15	0.67	0.08	0.39	0.15	0.44
		0.93	**3.65**	**0.23**	**0.41**	**0.22**	**0.78**	**0.13**	**0.46**	**0.22**	**0.51**
A4	**AS1**	0.98	1.17	0.09	0.18	0.16	0.22	0.06	0.11	0.07	0.12
		1.13	**0.78**	**0.11**	**0.12**	**0.18**	**0.15**	**0.07**	**0.06**	**0.08**	**0.08**
A6	**AS3**	3.4	0.62	0.57	0.08	0.78	0.12	0.49	0.04	0.53	0.05
		3.53	**0.26**	**0.56**	**0.04**	**0.82**	**0.08**	**0.51**	**0.01**	**0.55**	**0.02**
A8	**AS5**	1.02	1.03	0.19	0.24	0.21	0.25	0.1	0.14	0.14	0.18
		1.21	**1.27**	**0.21**	**0.3**	**0.24**	**0.31**	**0.12**	**0.18**	**0.15**	**0.24**
E1	**AU1**	2.82	1.15	0.48	0.16	0.68	0.21	0.42	0.1	0.46	0.11
		3.9	**1.29**	**0.62**	**0.16**	**0.96**	**0.23**	**0.60**	**0.11**	**0.65**	**0.12**
E3	**AU3**	3.2	2.75	0.35	0.37	0.49	0.56	0.29	0.32	0.33	0.36
		3.15	**3.04**	**0.46**	**0.39**	**0.71**	**0.62**	**0.43**	**0.36**	**0.47**	**0.4**
E5	**AU5**	2.4	0.9	0.35	0.18	0.55	0.19	0.32	0.09	0.36	0.13
		3.3	**0.9**	**0.43**	**0.18**	**0.78**	**0.19**	**0.46**	**0.09**	**0.52**	**0.13**
AF1		1.11		0.15		0.2		0.09		0.1	
		1.2		0.16		0.21		0.09		0.11	

were considered to be the most promising ones, as can be noticed in Fig. 2. Points A8, AF4 and AS2 present higher percentages, which can reach a maximum of 14% during the total time and 13% in winter, noting that the values are distributed along a narrower *Hs* interval, especially in the case of point AS2. For the remaining points, it can be mentioned that A6 presents a more significant distribution between the isolines 25–100 kW/m; AF3 is defined by a flattened distribution, which can reach periods of 12 s; and AU4 presents more important values in the intervals of 1.5–4 m and 6.5–10.5 s

To better visualize the variation of the wave energy resource with the significant wave height and the wave energy period, the data from some relevant sites (corresponding to the four reference points defined in Fig. 3b—A1, E4, A6 and AU4) are also presented in the form of trivariate diagrams that combine the scatter and the wave energy diagrams [64–66]. The number in each square indicates the occurrence of the corresponding sea states in terms of number of hours in the average year (defined as the average of the 15-year dataset considered). The colour indicates the contribution of the different sea states to the total annual wave energy at the point considered. The annual average scatter diagrams for four sites are presented in Figs. 8 and 9 for the two reference points corresponding to the northern and the southern hemispheres, respectively.

3.2. WEC performance

Another objective of the present work was to assess the performance of the WECs presented in Table 2. Similarly to the wind industry, in which the performance of wind turbine is obtained by combining the specific power curve with the wind measurements, in the case of a WEC generator, a power matrix (defined by the manufacturer) is used. This is combined with the bivariate distributions (*Hs* × *Te*) presented in Figs. 6 and 7. The corresponding mathematical expression [5,26] can be defined as

$$P_E = \frac{1}{100} \cdot \sum_{i=1}^{nT} \sum_{j=1}^{nH} PW_{ij} \cdot PM_{ij}, \tag{6}$$

where PW_{ij} is related to the bivariate distribution and includes the bin defined by column j and line i, whereas PM_{ij} is the expected power output defined in the power matrix of each WEC for the same bin (defined by column j and line i).

A common way to determine the power matrix of the WECs is through numerical simulations, which are validated in some cases by real field experiments, as in the case of the Pelamis system. At this point, we can also highlight the fact that most of the devices considered are only in the development stage, so the rated power can significantly

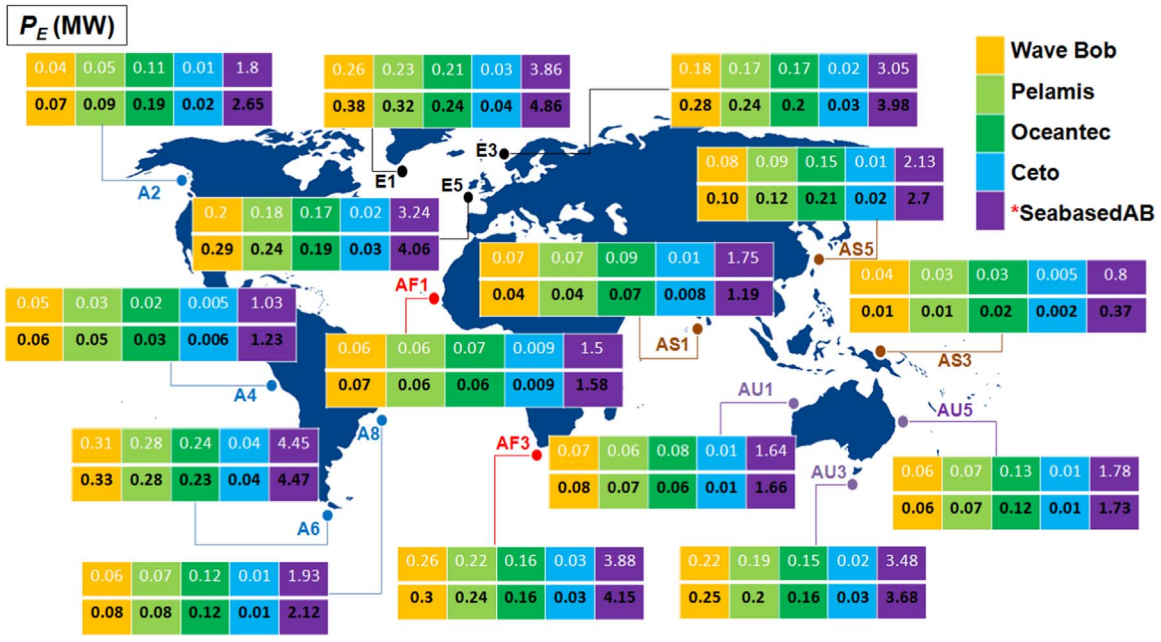

Fig. 11. Power output (in MW) expected from the WECs rated below 1000 kW. Mean values correspond to the 15-year interval from January 2000 to December 2014, where the first and second lines of each table indicates the WEC performance during the total and winter times, respectively. The output of the SeabasedAB system was expressed in kW.

Table 5
Power output (in MW) expected from the WECs rated below 1000 kW, indicated in terms of the mean values corresponding to the 15-year interval from January 2000–December 2014. The output of the SeabasedAB system is expressed in kW, and the wintertime values are highlighted.

Point		Wave Bob		Pelamis		Oceantec		Ceto		SeabasedAB (in kW)	
A1	**AF2**	0.18	0.06	0.18	0.04	0.2	0.02	0.03	0.005	3.3	1.1
		0.27	**0.07**	**0.25**	**0.04**	**0.25**	**0.02**	**0.04**	**0.006**	**4.2**	**1.2**
A3	**AF4**	0.07	0.03	0.04	0.04	0.026	0.11	0.006	0.01	1.22	1.7
		0.05	**0.04**	**0.03**	**0.05**	**0.021**	**0.13**	**0.005**	**0.02**	**0.96**	**1.82**
A5	**AS2**	0.14	0.07	0.12	0.05	0.11	0.05	0.02	0.007	2.55	1.38
		0.16	**0.08**	**0.14**	**0.06**	**0.12**	**0.05**	**0.02**	**0.008**	**2.76**	**1.57**
A7	**AS4**	0.06	0.06	0.07	0.06	0.12	0.07	0.01	0.01	1.8	1.38
		0.07	**0.1**	**0.08**	**0.1**	**0.12**	**0.12**	**0.02**	**0.02**	**1.9**	**2.21**
A9	**AS6**	0.19	0.16	0.19	0.16	0.21	0.18	0.03	0.02	3.43	3
		0.29	**0.25**	**0.27**	**0.23**	**0.26**	**0.24**	**0.04**	**0.03**	**4.43**	**4**
E2	**AU2**	0.24	0.18	0.21	0.14	0.2	0.1	0.03	0.02	3.62	2.9
		0.34	**0.21**	**0.3**	**0.16**	**0.22**	**0.1**	**0.04**	**0.02**	**4.6**	**3.15**
E4	**AU4**	0.2	0.24	0.17	0.23	0.14	0.25	0.02	0.03	3.11	4.1
		0.28	**0.27**	**0.23**	**0.26**	**0.16**	**0.25**	**0.03**	**0.04**	**3.9**	**4.31**
E6		0.08		0.06		0.07		0.01		1.61	
		0.12		0.09		0.07		0.01		2.1	

increase. In this work, the rated powers (*RP*) were considered as the maximum values from the power matrix reported in the literature review, but these values may change with the evolution of the WEC industry. By using this theoretical approach to investigate the power output, a realistic estimation can be obtained. Nevertheless, this approach does not consider the conditions when the system will lose energy throughout the power-take-off system or will be shut down for maintenance. However, by using large periods of reanalysis wave data, it is possible to reduce the uncertainties coming from the inter-annual variations of the wave resources.

From this perspective, Fig. 10 presents the expected power output (in MW) of the WECs rated above 2500 kW, considering only fifteen reference points. The results correspond to the 15-year interval (2000–2014) and are structured in total and winter times (second line). As can be observed, the Wave Dragon system presents higher values in the conditions when defined by a higher rated power, whereas in terms of the reference points, the most promising areas seems to be near E2, E4, E6, AU4, A9, AS6 and A5. Reported over the total time, the Wave Dragon presents values of 2.73 MW, 2.45 MW and 1.21 MW in E2, E4 and E6, respectively, whereas from the northern American region A9 with 2.23 MW and A1 with 2.17 MW can be mentioned. Point AS4 reports a lower value of 0.87 MW, which can exceed even AF4 by almost 0.23 MW. From the southern part, Wave Dragon may perform well in the Australian area, in points AU2 and AU4, where a maximum of 2.68 MW is observed, and also in A5, where 1.93 MW can be expected. From the remaining WECs, the Sea Power device presents the best performance, followed by the PPC system, the Wave Star and the OE device. Following this order, during the total time, these systems present electric power values in the ranges: A1→0.3–0.5 MW, A5→0.19–0.36 MW, A9→0.32–0.52 MW, E4→0.31–0.54 MW, AF2→0.06–0.16 MW, AS4→0.09–0.19 MW or AU4→0.38–0.61 MW. During wintertime, the power output of the WECs (including the Wave Dragon) can be associated with A3→0.06–1 MW, A7→0.11–1.06 MW, E2→0.52–3.75 MW, AF4→0.07–0.75 MW, AS2→0.1–1.35 MW or AU2→0.28–2.82. For point AU2, the OE and Wave Star systems may perform better than the PPC generator.

A similar analysis is presented in Table 4 for the remaining points. For the Wave Dragon system, more important values can be mentioned in the points A6→3.4/3.53 MW (total/winter), AF3→3.24/3.65 MW, E3→3.2/3.15 MW and E5, which during wintertime may report a value

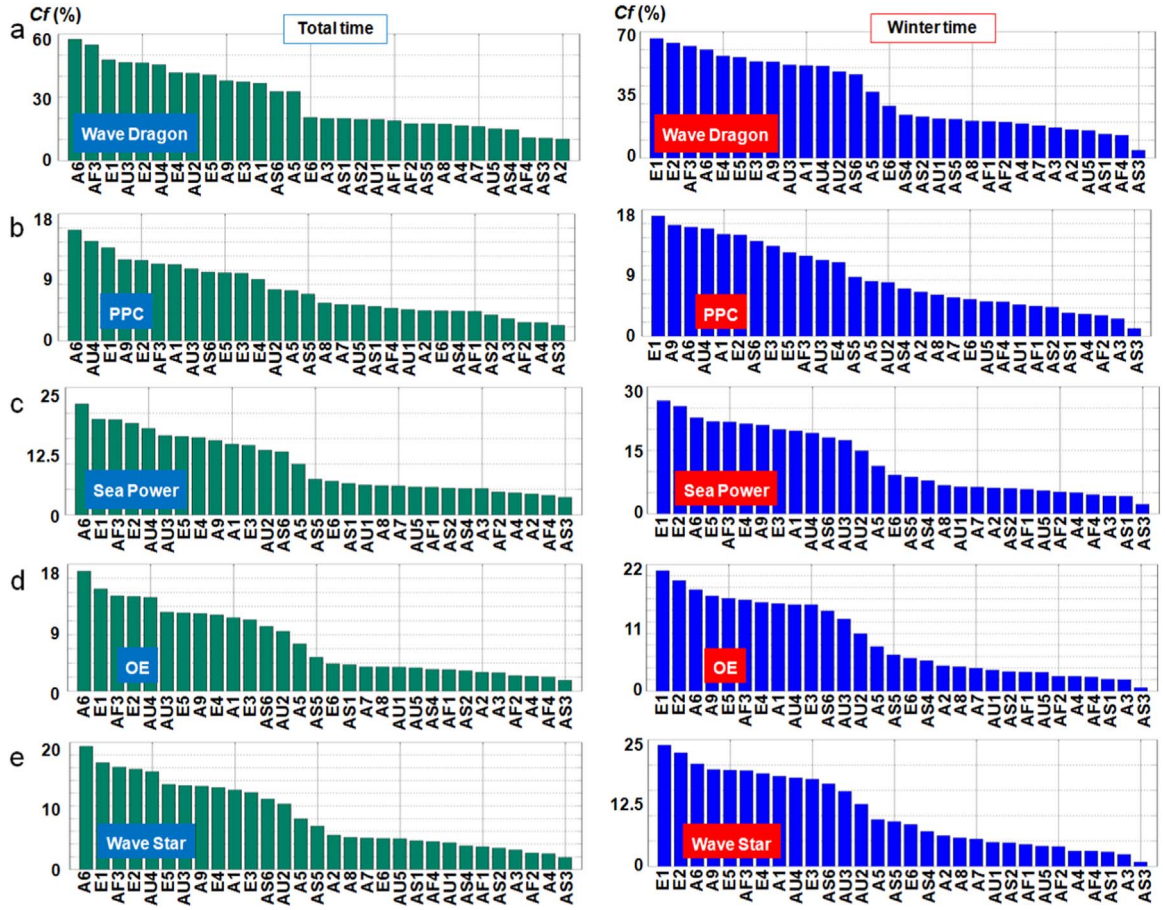

Fig. 12. Capacity factor (%) of the WECs rated above 2500 kW based on the wave data from the interval from 2000 to 2014. The results correspond to the total/winter time intervals and are presented in descending order.

of 3.3 MW. Regarding the PPC system, it can be observed that during the total time, the values do not exceed 0.6 MW, whereas during winter 0.56 MW in A6 and 0.62 MW in E1 can be expected, and a minimum of 0.04 MW is encountered in AS3. The remaining WECs seem to perform better during the total time in point A6, where the systems report values of 0.78 MW (Sea Power), 0.53 MW (Wave Star) and 0.49 MW (OE) compared with wintertime, when the values corresponding to point E1 may increase to 0.96 MW, 0.65 MW and 0.6 MW, respectively.

Fig. 11 presents the expected power output for the systems rated below 1000 kW, noting that the values corresponding to the SeabasedAB system are expressed in kW. Regarding the northern region, higher values occur in E1, compared with the Southern Hemisphere where points A6, AF3 or AU3 seem to be more productive. The differences noticed among the first three systems (Wave Bob, Pelamis and Oceantec) are small, with each system presenting various performance. For example, the Wave Bob system may perform well in A4, AF3 or AU3, whereas Oceantec has better performance in A2, A8, AS5 or AU5. During the total and winter times, these three systems have values in the intervals A2→0.04–0.11 MW/0.07–0.19 MW; A6→0.06–0.12 MW/0.08–0.12 MW, E3→0.21–0.26 MW and AS5→0.08–0.15 MW/0.1–0.21 MW. The Ceto system presents values in the range of 0.009–0.04 MW, with better performance in A6 and E1, noting that wintertime presents similar values. The performance of this system is slightly higher than that reported by the SeabasedAB generator, which during the total time has power values of 4.45 kW in A6, 3.24 kW in E5 and 3.48 kW in AU3. The values reported during wintertime are in the range of 0.37–4.86 kW, with better results corresponding to the points located near the European coasts.

Table 5 presents the performance of these systems for the remaining sites. The results from this table show that the WECs appear to have better outputs in reference points E2 and AU4, whereas much lower performance corresponds to reference point AF4.

4. Discussion

In this section, the performance of the WECs will be discussed considering some synthetic parameters. The first parameter to be assessed and discussed is the capacity factor (C_f). This is expressed in % and defined as

$$C_f = 100 \cdot \frac{P_E}{RP}, \tag{7}$$

where P_E is the electric power expected to be generated by each WEC, and RP represents the rated power of each system according to the values presented in Table 2.

Fig. 12 presents the distribution of this parameter for the WECs rated above 2500 kW, considering the 15 years of ECMWF data, which were structured in total and winter time, respectively. The results were ordered from highest to lowest values, with the first points representing the sites where the system considered presents better performance. From the analysis of the Wave Dragon device, we can notice that during the total time, the first five positions correspond to points A6, AF3, E1, AU3 and E2, which have values in the range of 46.3–57.5%. The next five positions correspond to AU4, E4, AU2, E5 and A9, with values between 37.8% and 45.4%. On the opposite side, points AU5, AS4, AF4, AS3 and A2, can be found, which do not exceed 15.2%. These values increase during wintertime, reaching a maximum of 66.1% in E1, which is followed by E2 and AF3 with 63.6% and 61.9%, respectively, and a minimum of 4.43% can be noticed in the vicinity

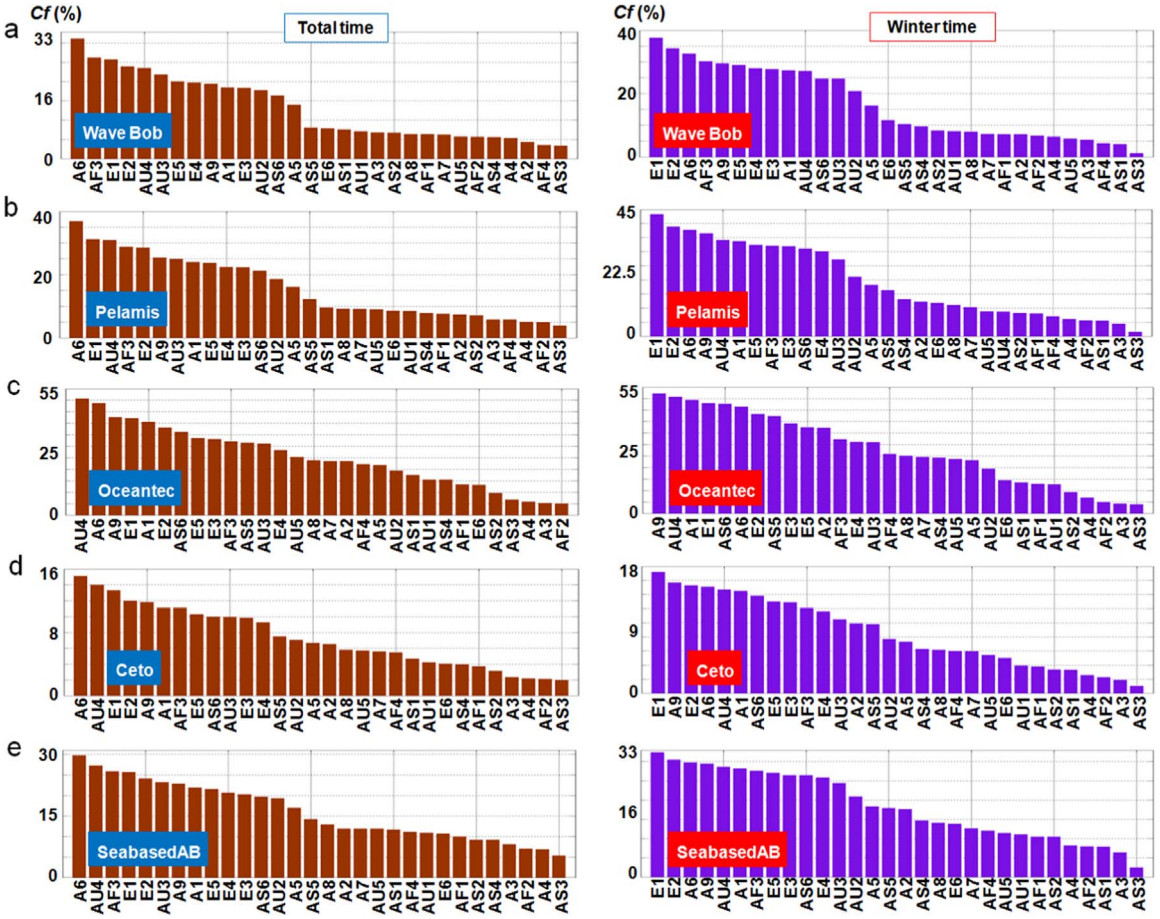

Fig. 13. Capacity factor (%) of the WECs rated below 1000 kW based on the wave data from the interval from 2000 to 2014. The results correspond to the total/winter time intervals and are presented in descending order.

of AS3.

Lower values correspond to the rest of the WECs in this group, although the distribution of the points remains quite similar. For the PPC system, points A6, AU4, E1 and A9 present the most important values, which during the total time are in the range of 11.4–15.7%, compared with winter when the interval is shifted to 14.5–17.1%. In this case, the lowest values found in several points from America, Africa and Asia with a minimum of 2.22% during the total time and 1.11% in winter. The Sea Power presents a maximum of 21.8% in A6 and 26.7% in E1 during the total time, whereas group points AS5–AS3 do not generally exceed 7.1% compared with the value 8.8%, which can be expected in winter.

During the total time, the OE system presents a distribution similar to that corresponding to the PPC generator, whereas during winter, four European points can be found among the seven considered as the most energetic points with a maximum of 21% and a minimum of 15.4%. During the total time, the Wave Star generator presents a maximum of 19.4% in A6, followed by group points E1–AU2, where the values gradually decrease from 16.8–10.3%; the rest of the points have capacity factors with values below 8%. The winter distribution is dominated by point E1 with 23.9%, which is subsequently defined by some other reference points, such as E3 (17.5%), A8 (5.61%) and AS3 (0.87%).

Going to the WECs rated below 1000 kW, a similar analysis is presented in Fig. 13. From the analysis of the maximum values, it can be mentioned that except for the Ceto device, the rest of the systems present better performance than the systems rated above 2500 kW. From this perspective, the Oceantec device presents values that are comparable with the Wave Dragon, especially during the total time. The capacity factor has a maximum of 31.2% in A6 during the total time, with values decreasing from 26.3–14% for the group AF3–A5, whereas the rest of the sites do not exceed 8%. In winter, group points E1–E5 account for the first positions, reaching a maximum of 37.6% in E1, whereas lower values are noticed near AS1 and AS3, where a minimum of 1.22% is encountered.

During the total time, the Pelamis system seems to perform better in A6 with 36.9%, followed by E1 (31.2%), AU4 (30.9%) and AF3 (28.8%), and the lowest performance is encountered in reference points AF2 (5%) and AS3 (3.9%). During wintertime, this system has much higher values for the sites from Europe (E1 and E2) and America (A6 and A9) presenting a maximum of 43.3% and a minimum of 36.5%. The Oceantec device indicates better performance for point AU4 and several points from America (A1, A6 and A9) and even for reference point AS6 corresponding to the Asian region, which during wintertime may reach a maximum value of 47.7%. The Ceto device accounts for the lowest values, which may reach maximum values in America of 15.7% (A9), Europe of 17.2% (E1), Africa of 12.1% (AF3), Asia of 13.8% (AS6) and Australia of 14.7% (AU4). The SeabasedAB device presents higher values for points A6, AU4, AF3, E1 and E3 during the total time, compared with the winter season, when these positions are occupied by reference points E1, E2, A1, A6, and A9 and also by AU4.

Another important parameter is the capture width (in m), which is used to estimate the portion of the wave front from which it is considered that a WEC system generates power [26]. This parameter can be defined as

$$C_W = \frac{P_E}{P_W}, \tag{8}$$

where P_E is the WEC power output for each site, and P_W is the wave power for the same location. Only the mean values of both parameters

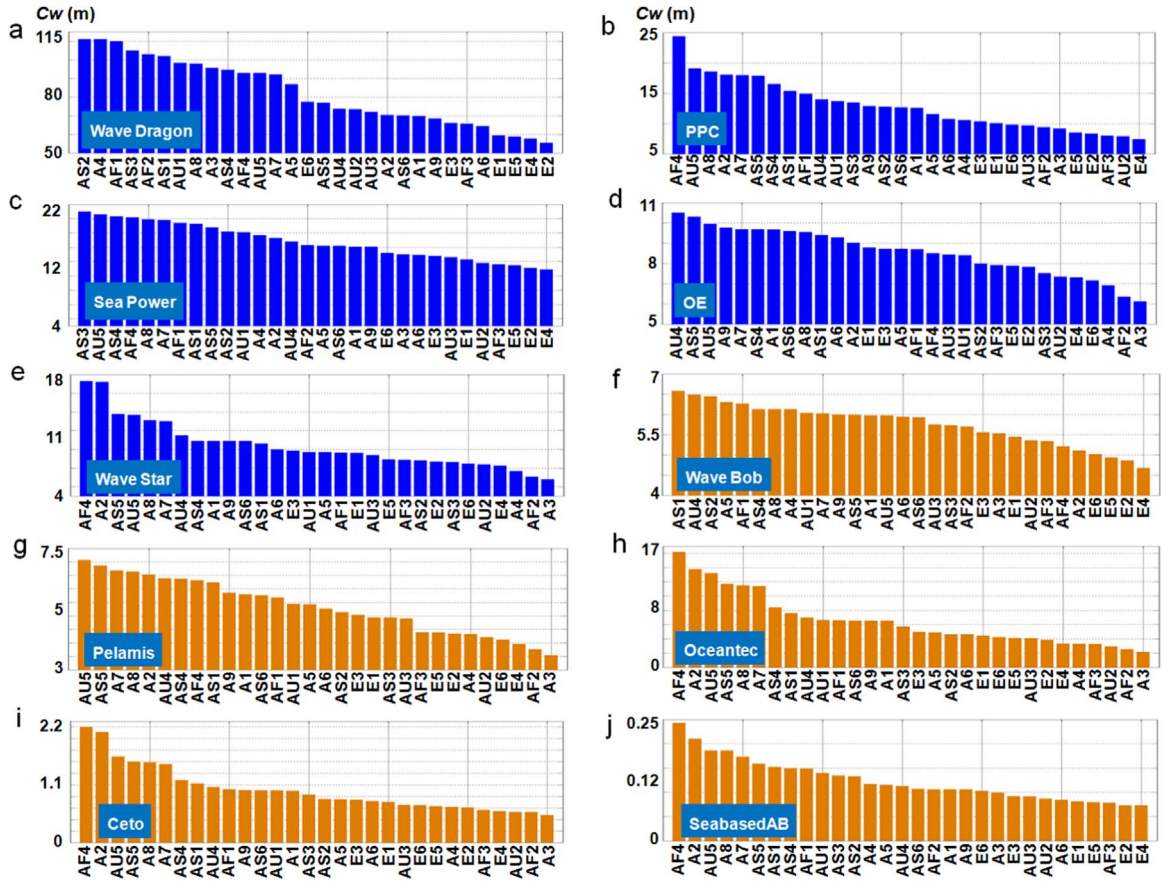

Fig. 14. Capture width (m) of the WECs corresponding to the total time for the interval from 2000 to 2014: a–e) systems rated above 2500 kW; f–j) systems rated below 1000 kW. The results are presented in descending order.

are considered. Regarding this parameter, it can be mentioned that a site with moderate wave energy may have a higher capture width, which may bring into discussion the use of the WEC systems in the coastal sectors where the erosion processes represent a real problem, as in the case of the enclosed seas [16,67].

Fig. 14 presents the evolution of this index for all WECs by considering only the total time period. The Wave Dragon presents the highest values, the PPC and Sea Power seem to be in the same category, and the maximum values of 2.2 m and 0.25 m are reported by Ceto and SeabasedAB, respectively. If we analyse the distribution of the values, a reverse trend can be observed, in the sense that the points that previously reported higher values for the power output or for the capacity factor have lower values. This should not necessarily be considered as a negative aspect because it might be interpreted that the WECs use the wave front more efficiently, by extracting more energy from a smaller area.

The Wave Dragon covers a significant part of the wave front in Asia (AS1, AS2 and AS3), Africa and America (A4), and it will be more efficient in areas located near points E1–E5, where only a 55.5 m wave front will be necessary, compared with 111 m corresponding to reference point AS2. Regarding the PPC system, the following reference points can be mentioned: AF4 (24.4 m), AU4 (14 m), A6 (10.8 m) and E4 (7.4 m). The Sea Power system presents a constant decreasing trend of the capture width values from a maximum of 21 m (AS3), including 16.8 m (AU4) and finally reaching a minimum of 12.9 m in E4, which can be considered to be one of the highest values if we exclude the Wave Dragon.

The OE system and the Wave Star generally present capture width values in the ranges of 10.5–6.13 m and 17.3–6.8 m, respectively. It should be noted, however, that in the case of the OE system, group points A6–A3 (18 points) do not exceed the value of 10 m for the capture width.

Regarding the WECs rated below 1000 kW, it can be observed that from this point of view, the Wave Bob has better performance in the Asian regions (AS1, AS2 and AS4), where a maximum of 6.58 m is noticed; this is also the case for sites AU4 and AF1, compared with the European sites where a minimum capture width value of 4.7 m is encountered. The Ceto device shows values in the range of 1.36–2 m for points A9–A7, whereas for the rest of the points, the capture width does not exceed 1.1 m.

5. Conclusions

Motivated by the fact that the wave energy market has the potential to exceed the offshore wind industry by 2050 and significantly contribute to the future energy mix [68], in the present work, a review of the wave energy potential was carried out on a global scale, and the performance of some state-of-the-art WECs were assessed worldwide. The analyses were performed by considering the reanalysis wave data provided by the European Centre for Medium-Range Weather Forecasts for the 15-year interval of 2000–2014.

Following the current trends reported in the WEC industry, it can be mentioned that most of the research activities are focused on projects that involve point absorber systems; this aspect is considered by the manufacturers of the Wave Star and PPC systems, which use multiple point absorbers. These types of systems could be considered to be more suitable for the European areas located in the Northern Hemisphere if we consider that these regions are under the influence of the swells coming alternatively from the North Atlantic and Arctic Oceans. Following the global areas identified with the highest wave power density, thirty reference points (for both hemispheres) were defined. These are considered to present the most suitable conditions

for the development of various offshore projects. The large scale of WEC devices considered enables the determination of the performance of a broader range of generators from those available in the market in conditions when some of these projects were shut down while many others are dynamically evolving.

From the analysis of the wave conditions, the facts were highlighted that the points from the Northern Hemisphere present more significant variations in winter conditions and that the wave conditions may also present consistent inter-annual variations, which are more severe in the European regions. Usually, during wintertime, more energetic values are noticed, but this is not the case for points A3, AS1 or AS3, which do not follow this trend. The wave rise representations clearly indicate the generation area for each coastal environment, also proving the accuracy of the ERA-Interim database to assess this wave parameter.

By combining the bivariate distribution of the sea states corresponding to each site with the power matrices of each WEC mentioned in Table 2, it was possible to evaluate the expected power output in megawatts, with the exception of the SeabasedAB system, which presents lower values in the range of 0.8–4.45 kW (total time) and 0.37–4.86 kW (in winter). From the WEC systems rated above 2500 kW, the Wave Dragon presents the best performance in terms of the power output, capacity factor and capture width. From the WECs rated below 1000 kW, the devices Wave Bob, Pelamis and Oceantec show small variations between the power output compared with the capacity factor and capture width index, in which the Oceantec stands out with a maximum C_f value of 55.2% (for A2) and a C_w value of 16.2 m (for AF4).

Finally, it can also be mentioned that the wave energy sector is a very dynamic one, and the near future of this industry will most likely be related to the implementation of various hybrid projects.

Acknowledgments

This work was supported by a grant of the Romanian Ministry of National Education, CNCS—UEFISCDI PN-II-ID-PCE-2012-4-0089 (project DAMWAVE). The work of the second author has been funded by the Sectoral Operational Programme Human Resources Development 2007–2013 of the Ministry of European Funds through the Financial Agreement POSDRU/159/1.5/S/132397.

ECMWF ERA-Interim data used in this study have been obtained from the ECMWF data server.

References

[1] Kim G, Lee ME, Lee KS, Park J-S, Jeong WM, Kang SK, Soh J-G, Kim H. An overview of ocean renewable energy resources in Korea. Renew Sustain Energy Rev 2012;16:2278–88.
[2] Zanuttigh B, Angelelli E, Kortenhaus A, Koca K, Krontira Y, Koundouri P. A methodology for multi-criteria design of multi-use offshore platforms for marine renewable energy harvesting. Renew Energy 2016;85:1271–89.
[3] Zabihian F, Fung Alan S. Review of marine renewable energies: case study of Iran. Renew Sustain Energy Rev 2011;15(5):2461–74.
[4] Wang SJ, Yuan P, Li D, Jiao YH. An overview of ocean renewable energy in China. Renew Sustain Energy Rev 2011;15(1):91–111.
[5] Rusu L, Onea F. Assessment of the performances of various wave energy converters along the European continental coasts. Energy 2015;82:889–904.
[6] Morim J, Cartwright N, Etemad-Shahidi A, Strauss D, Hemer M. A review of wave energy estimates for nearshore shelf waters off Australia. Int J Mar Energy 2014;7:57–70.
[7] MAJR Quirapas, Lin H, MLS Abundo, Brahim S, Santos D. Ocean renewable energy in Southeast Asia: a review. Renew Sustain Energy Rev 2015;41:799–817.
[8] Rusu E, Onea F. Study on the influence of the distance to shore for a wave energy farm operating in the central part of the Portuguese nearshore. Energy Convers Manag 2016;114:209–23.
[9] Uihlein A, Magagna D. Wave and tidal current energy – A review of the current state of research beyond technology. Renew Sustain Energy Rev 2016;58:1070–81.
[10] Hadzic N, Kozmar H, Tomic M. Offshore renewable energy in the Adriatic Sea with respect to the Croatian 2020 energy strategy. Renew Sustain Energy Rev 2014;40:597–607.
[11] Onea F, Raileanu A, Rusu E. Evaluation of the wind energy potential in the coastal environment of two enclosed seas. Adv Meteor 2015;2015:14.
[12] Onea F, Rusu E. Wind energy assessments along the Black Sea basin. Meteorol Appl 2014;21(2):316–29.
[13] Alamian R, Shafaghat R, Miri SJ, Yazdanshenas N, Shakeri M. Evaluation of technologies for harvesting wave energy in Caspian Sea. Renew Sustain Energy Rev 2014;32:468–76.
[14] Arena F, Laface V, Malara G, Romolo A, Viviano A, Fiamma V, et al. Wave climate analysis for the design of wave energy harvesters in the Mediterranean Sea. Renew Energy 2015;77:125–41.
[15] Besio G, Mentaschi L, Mazzino A. Wave energy resource assessment in the Mediterranean Sea on the basis of a 35-year hindcast. Energy 2016;94:50–63.
[16] Rusu L. Assessment of the Wave Energy in the Black Sea Based on a 15-Year Hindcast with Data Assimilation. Energies 2015;8(9):10370–88.
[17] Onea F, Rusu E. Efficiency assessments for some state of the art wind turbines in the coastal environments of the Black and the Caspian seas. Energy Explor Exploit 2016;34(2):217–34.
[18] Cradden L, Kalogeri C, Martinez Barrios I, Galanis G, Ingram D, Kallos G. Multi-criteria site selection for offshore renewable energy platforms. Renew Energy 2016;87:791–806.
[19] Angelis-Dimakis A, Biberacher M, Dominguez J, Fiorese G, Gadocha S, Gnansounou E, et al. Methods and tools to evaluate the availability of renewable energy sources. Renew Sustain Energy Rev 2011;15:1182–200.
[20] Alonso R, Solari S, Teixeira L. Wave energy resource assessment in Uruguay. Energy 2015;93:683–96.
[21] Zanuttigh B, Elisa Angelelli E. Experimental investigation of floating wave energy converters for coastal protection purpose. Coast Eng 2013;80:148–59.
[22] Kramer M, Marquis L, Frigaard PKramer M, MarquisL, FrigaardP.Performance Evaluation of the Wavestar Prototype. In A. S. BahajA. S. Bahaj (Ed.), 9th EWTEC 2011: In: Proceedings of the 9th EWTEC 2011: 9th European Wave and Tidal Conference, Southampton, UK, 5th-9th September 2011. University of Southampton.
[23] Rusu L, Guedes Soares C. Wave energy assessments in the Azores islands. Renew Energy 2012;45:183–96.
[24] Monteforte M, Lo ReC, Ferreri GB. Wave energy assessment in Sicily (Italy). Renew Energy 2015;78:276–87.
[25] Fadaeenejad M, Shamsipour R, Rokni SD, Gomes C. New approaches in harnessing wave energy: with special attention to small islands. Renew Sustain Energy Rev 2014;29:345–54.
[26] Rusu E, Onea F. Estimation of the wave energy conversion efficiency in the Atlantic Ocean close to the European islands. Renew Energy 2016;85:687–703.
[27] Dee DP, Uppala SM, Simmons AJ, Berrisford P, Poli P, Kobayashi S, et al. The era-Interim reanalysis: configuration and performance of the data assimilation system. Q J R Meteorol Soc 2011;137:553–97.
[28] Lawrence J, Sedgwick J, Jeffrey H, Bryden I. An overview of the UK Marine energy sector. Proc IEEE 2013;101(4):876–90.
[29] Leybourne M, Batten WMJ, Bahaj AS, Minns N, O'Nians J. Preliminary design of the OWEL wave energy converter pre-commercial demonstrator. Renew Energy 2014;61:51–6.
[30] Falcao AFO. Modelling of wave energy conversion. Instituto Superior Técnico, Universidade Técnica de Lisboa; 2014.
[31] Lopez I, Andreu J, Ceballos S, Martínez de Alegría I, Kortabarria I. Review of wave energy technologies and the necessary power-equipment. Renew Sustain Energy Rev 2013;27:413–34.
[32] Cuadra L, Salcedo-Sanz S, Nieto-Borge JC, Alexandre E, Rodríguez G. Computational intelligence in wave energy: comprehensive review and case study. Renew Sustain Energy Rev 2016;58:1223–46.
[33] Mackay EBL, Bahaj AS, Challenor PG. Uncertainty in wave energy resource assessment. Part 1: historic data. Renew Energy 2010;35(8):1792–808.
[34] Mackay EBL, Bahaj AS, Challenor PG. Uncertainty in wave energy resource assessment. Part 2: variability and predictability. Renew Energy 2010;35(8):1809–19.
[35] Astariz S, Iglesias G. The economics of wave energy: a review. Renew Sustain Energy Rev 2015;45:397–408.
[36] Onea F, Rusu E. The expected efficiency and coastal impact of a hybrid energy farm operating in the Portuguese nearshore. Energy 2016;97:411–23.
[37] Perez-Collazo C, Greaves D, Iglesias G. A review of combined wave and offshore wind energy. Renew Sustain Energy Rev 2015;42:141–53.
[38] Karimirad M. Offshore energy structures: for wind power wave energy and hybrid marine platforms. Berlin, Germany: Springer; 2014.
[39] Zanopol AT, Onea F, Rusu E. Coastal impact assessment of a generic wave farm operating in the Romanian nearshore. Energy 2014;72:652–70.
[40] Zanopol AT, Onea F, Rusu E. Evaluation of the coastal influence of a generic wave farm operating in the Romanian nearshore. J Environ Prot Ecol 2014;15(2):597–605.
[41] Mendoza E, Silva R, Zanuttigh B, Angelelli E, Andersen TL, Martinelli L, Nørgaard JQH, Ruol P. Beach response to wave energy converter farms acting as coastal defence. Coast Eng 2014;87:97–111.
[42] Ilyas A, Kashif SAR, Saqib MA, Asad MM. Wave electrical energy systems: implementation, challenges and environmental issues. Renew Sustain Energy Rev 2014;40:260–8.
[43] European Centre for Medium Range Weather Forecasts. IFS Documentation – Cy40r1 Operational implementation, ECMWF wave model, 22 November 2013, p. 79.
[44] Mooney PA, Mulligan FJ, Fealy R. Comparison of ERA-40, ERA-Interim and NCEP/NCAR reanalysis data with observed surface air temperatures over Ireland. Int J Climatol 2011;31:545–57.
[45] PAEM Janssen. The interaction of ocean waves and wind. Cambridge, UK:

Cambridge University Press; 2004.
[46] Bahaj AS. Generating electricity from the oceans. Renew Sustain Energy Rev 2011;15:3399–416.
[47] Hammar L, Ehnberg J, Mavumec A, Cuamba BC, Molander S. Renewable ocean energy in the Western Indian Ocean. Renew Sustain Energy Rev 2012;16:4938–50.
[48] Lopez M, Veigas M, Iglesias G. On the wave energy resource of Peru. Energy Convers Manag 2015;90:34–40.
[49] EWEA. Deep water - The next step for offshore wind energy. A report by the European Wind Energy Association - July; 2013.
[50] Joubert JR, Johannes van Niekerk L, Reinecke J, Meyer I. Wave energy converters (WECs). Cent Renew Sustain Energy Stud 2013.
[51] Babarit A, Hals J, Muliawan MJ, Kurniawan A, Moan T, Krokstad J. Numerical benchmarking study of a selection of wave energy converters. Renew Energy 2012;41:44–63.
[52] Mann LD. Application of Ocean Observations & Analysis: The CETO Wave Energy Project. Operational Oceanography in the 21st Century: p. 721–729; 2011.
[53] Ocean Energy AS. The waves of the future. Report September 2014.
[54] Holmberg P, Andersson M, Bolund B, Kerstin S. Annual report: Implementing agreement on ocean energy systems; 2014.
[55] Rusu E. Assessment of the wave energy conversion patterns in various coastal environments.Energies, Special Issue Selected Papers from In: Proceedings of the 1st International e-Conference on Energies; 7(6): p. 4002–4018; 2014.
[56] Sea Power. ⟨http://www.seapower.ie/about/⟩ [accessed on June 2015]
[57] Sea Power Ltd. SeaPower Platform Configuration Test Program. Infrastructure Access Report 2014.
[58] Marquis L Kramer L Frigaard M. P. First Power Production figures from the Wave Star Roshage Wave Energy Converter. 3rd International Conference on Ocean Energy, 6 October, Bilbao; 2010.
[59] Scott A. Pelamis – Full scale development programme. International Conference on Ocean Energy. November 4-6. Halifax, Nova Scotia Canada; 2014.
[60] Environmental Change Institute. Variability of UK Marine Resources. Oxford, UK, 2005.
[61] EKINBERRI. OCEANTEC-Desarrollo tecnologico de un sistema de aprovechamiento de la energia de las olas. Informe publicable, 2006.
[62] Ruiz-Minguela P. Progress in the Development of OCEANTEC Wave Energy Converter.In: Proceedings of the Third International Symposium on Ocean Energy 2nd April, Bilbao Spain; 2009.
[63] Frigaard P, Kofoed JP, Knapp W. Wave Dragon: wave power plant using low-head turbines. In Hidroenergia 04: International Conference and Exhibition on Small Hydropower; 2004.
[64] Carballo R, Iglesias G. A methodology to determine the power performance of wave energy converters at a particular coastal location. Energy Convers Manag 2012;61:8–18.
[65] Veigas M, Carballo R, Iglesias G. Wave and offshore wind energy on an island. Energy Sustain Dev 2014;22:57–65.
[66] Iglesias G, Carballo R. Offshore and inshore wave energy assessment: Asturias (N Spain). Energy 2010;35:1964–72.
[67] Rusu E, Onea F. Evaluation of the wind and wave energy along the Caspian Sea. Energy 2013;50:1–14.
[68] SI OCEAN. Wave and tidal energy market deployment strategy for Europe. Intelligent Energy Europe Programme of the European Union. June 2014, p. 47.